Challenges of diagnosing glaucoma in myopic eyes

Qiu, Kunliang

Publication date:
2018

Chapter 4

Application of the ISNT rules on retina nerve fiber layer thickness and neuroretinal rim area in healthy myopic eyes

Kunliang Qiu, Geng Wang, Xuehui Lu, Riping Zhang, Lixia Sun, Mingzhi Zhang

Acta Ophthalmol. 2018 Mar;96(2):161-167.

ABSTRACT

Purpose: We determined the applicability of ISNT (inferior > superior > nasal > temporal) rules on RNFL thickness and rim area, and evaluated the impact of various ocular factors on the performance of the ISNT rules in healthy myopic eyes.

Methods: A total of 138 eyes from 138 healthy myopic subjects were included in this cross-sectional observational study. The peripapillary retinal nerve fiber layer (RNFL) and optic disc in each eye were imaged with Cirrus HD OCT and Heidelberg Retina Tomograph II, respectively. The performance of the IS (inferior > superior), IST (inferior > superior > temporal), and ISNT rules on RNFL thickness and rim area were determined and compared between low to moderate myopia and high myopia. The effects of ocular factors (including axial length, disc area, disc tilt, disc torsion, disc-fovea angle (DFA), and retina artery angle) on the performance of ISNT rules were evaluated with logistic regression analysis.

Results: The mean axial length and refractive error were 25.57±1.09 mm (range, 22.52 to 28.77 mm) and -5.12±2.30 D (range, -9.63 to -0.50 D), respectively. Sixty three percent of the healthy eyes were compliant with the ISNT rule on rim area, while ISNT rule on RNFL thickness was followed in only 11.6% of the included eyes. For rim area, smaller disc area was significantly associated with increased compliance of the IS rule (odds ratio: 0.46, $p=0.039$), IST rule (odds ratio: 0.46, $p=0.037$), and ISNT rule (odds ratio: 0.44, $p=0.030$). For RNFL thickness, greater DFA was significantly associated with increased compliance of the IS and IST rules (odds ratio: 1.30, $p<0.001$; odds ratio: 1.19, $p=0.006$, respectively).

Conclusions: In healthy myopic subjects, 88.4% and 37% of eyes did not comply with the ISNT rule on RNFL thickness and rim area, respectively. Due to significant low compliance in healthy eyes, the ISNT rule and its variants have limited potential utility in diagnosing glaucoma in myopic subjects.

Introduction

Glaucoma is a chronic and progressive optic neuropathy characterized by damage of retinal ganglion cells. Evaluation of structural damage of the optic nerve is important in glaucoma diagnosis. Jonas et al. first introduce the inferior > superior > nasal > temporal (ISNT) rule for glaucoma diagnosis (Jonas et al., 1988; Jonas et al., 1998). The ISNT rule states that the neuroretinal rim width is generally widest in the inferior (I) area, followed by the superior (S) and nasal (N) areas, narrowest in the temporal (T) area (Jonas et al., 1988). Although the rule has been widely used for glaucoma diagnosis, the application of the ISNT rule in clinical practice is generally conducted with ophthalmoscopy and, therefore, is a subjective assessment. With recent advances of the optical coherence tomography (OCT) technology and the confocal scanning laser ophthalmoscopy (CSLO), objective and quantity measurement of RNFL thickness and neuroretinal rim area has been shown emerging as an important diagnostic technology for glaucoma (Fallon et al., 2017). By using optic disc photographs, OCT technology, and the CSLO technology, the application of the ISNT rule on RNFL thickness and rim area has been tested in previous studies (Harizman et al., 2006; Sihota et al., 2008; Chan et al., 2013; Dave & Shah 2015; Hwang & Kim 2015; Pradhan et al., 2016). While some studies have found that the ISNT rule is clinical useful in differentiating normal from glaucomatous eyes (Harizman et al., 2006), others have reported that the ISNT rule has limited utility in the diagnosis of glaucoma (Sihota et al., 2008; Hwang & Kim 2015; Pradhan et al., 2016).

Myopia is a prevalent condition in Asia and a major risk factor for glaucoma (Marcus et al. 2011; Morgan et al. 2012). Thus, it is important to determine the applicability of ISNT rule in myopic eyes. However, there are few studies on the applicability of ISNT and IST rules in myopic eyes (Kim et al. 2014). By using optic disc photographs, the sensitivity (73.3% to 75.7%) and specificity (68.3% to 71.4%) of the ISNT rule in diagnosing glaucoma have been reported in eyes with myopic titled discs (Kim et al., 2014). To the best of our knowledge, there are no studies on the performance of ISNT rule in healthy myopia by using OCT and

CSLO devices. The purpose of the present study was to determine the applicability of ISNT rules to RNFL thickness and rim area obtained with OCT and CSLO in healthy myopic eyes. Several ocular factors have been reported to be associated with rim area measurement and RNFL distribution in myopic eyes (Oddone et al., 2009; Pereira et al., 2015). Therefore, a second objective of this study was to evaluate the impact of various ocular factors on the performance of the ISNT rule and its variants in myopic eyes.

Methods

Subjects

One hundred and forty seven healthy myopic subjects were consecutively recruited from the refractive surgery clinic of Joint Shantou International Eye Center. All the included subjects underwent a complete ophthalmic examination including the measurement of refraction, visual acuity, intraocular pressure (IOP), axial length (IOL master; Carl-Zeiss Meditec, Dublin, CA), and a dilated stereoscopic fundus examination. All the included eyes had no concurrent ocular disease, other than a refractive error (spherical equivalent less than -0.5 diopters (D)). All subjects were subdivided into two groups according to refractive status: high myopia group (spherical equivalent <-6 D) and low to moderate group (spherical equivalent between -0.50 and -6.00 D). Subjects were excluded if the best corrected visual acuity was less than 20/40, the IOP over 21 mmHg, if they had a family history of glaucoma, or if they had a history of myopic macular degeneration, diabetes, neurological disease, refractive surgery, intraocular surgery, or glaucoma. One eye from each subject was randomly selected for analysis. The present study followed the tenets of the declaration of Helsinki and was approved by the ethical committee of Joint Shantou International Eye Center. Written informed consent was obtained from each subject before enrolment.

Visual field testing

Visual field tests of all the included subjects were performed with standard automated perimetry using the 24-2 grid and the SITA standard strategy (Humphrey Field Analyzer II; Carl Zeiss Meditec, Inc.). Only reliable visual field tests (with false positive and negative less than 10%, and fixation loss less than 20%) were included in the present study. All the included visual field tests were within normal limits in the glaucoma hemifield test (GHT) and had a pattern standard deviation (PSD) p value > 5%.

Confocal scanning laser ophthalmoscopy imaging

The optic disc imaging was performed with confocal scanning laser ophthalmoscopy (Heidelberg Retina Tomograph II [HRT2]; Heidelberg Engineering, GmbH, Dossenheim, Germany). A three-dimensional topographic image is constructed from multiple focal planes axially along the optic nerve head. An average of three consecutive scans is obtained and aligned to construct a single topography for analysis. Each optic disc image was checked carefully for image quality. Only images with good quality (an average pixel height standard deviation no more than 30 μm) were included in the current analysis. All the contour lines were manually drawn by a trained ophthalmologist (KQ) based on the margin of the optic disc (defined as the inner edge of the Elschnig's ring).

Global neuroretinal rim area and 6 sectorial neuroretinal rim area measurements (temporal quadrant, superotemporal octant, inferotemporal octant, nasal quadrant, superonasal octant, and inferonasal octant) were calculated and exported from the build in software. In the present study, the superior neuroretinal rim was defined as the combination of the superonasal and superotemporal measurements, while the inferior neuroretinal rim was defined as the combination of the inferonasal and inferotemporal measurements. Disc area was also recorded for analysis.

Optical coherence tomography

Each of the included eyes underwent RNFL imaging with the Cirrus High Definition OCT (software version 5.0.0.326; Carl Zeiss Meditec, Dublin, CA). The scan speed for this OCT device is 27,000 A-scans per second and the axial resolution is 5 μm. The peripapillary RNFL measurement was performed with the Optic Disc Cube 200×200 protocol. OCT scans with eye movements during image acquisition (checked by reviewing the real-time SLO fundus images) were excluded and retaken. Each included image had minimum signal strength of 7. The RNFL thickness maps were derived from the analysis printout by the automatic built-in software. Average RNFL thickness and 4 quadrant RNFL thicknesses (superior, nasal, inferior, and temporal quadrant) were recorded for analysis.

Measurement of the disc-fovea angle (DFA)

Based on the coordinates of the fovea and the center of the optic disc, DFA was measured with the ImageJ software (available in the public domain at http://rsbweb.nih.gov/ij/; www.nih.gov, National Institutes of Health, Bethesda, MD, USA). The fovea was automatically detected by the OCT software with overplayed macular color thickness map on the SLO fundus image. By using Illustrator CS4 software (Adobe Systems Inc., San Jose, California), the RNFL thickness deviation map with disc center determined by the OCT software was exported and manually registered to the SLO fundus image. To make a good registration, the retinal vessel trajectories were used as a reference and the transparency of the optic disc image was set to 50% to allow visualization of the underlying SLO fundus image.

The DFA, defined as the angle between the disc-fovea line and the horizontal line, was then measured with ImageJ software on the overlaid images (Figure 1A) (Amini et al. 2014). A positive DFA value indicates that the fovea is located inferiorly with respect to the optic disc center.

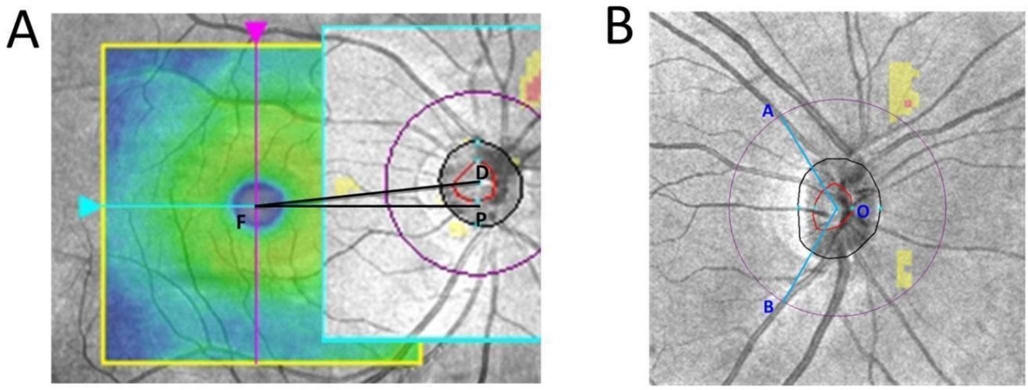

Figure 1. Measurements of disc-fovea angle (DFA) and retinal artery angle.
(A): Measurement of DFA on SLO fundus image. The fovea (point F) was automatically detected by the OCT software on the SLO fundus image with the macular color thickness map. The enface optic disc image (RNFL deviation map) with the optic disc center labelled (point D) by the OCT software was manually registered to the SLO fundus image with Illustrator CS4 software using the retinal vessels as reference. The DFA was defined as the angle between the disc-fovea line and the horizontal line (∠DFP).
(B): Measurements of retinal artery angle. The intersections (A and B) of the major temporal retinal artery and the 3.46 mm measurement circle were manually determined. The disc center (O) was automatically set by the OCT software. Artery angle was defined as ∠AOB.

Measurement of major retinal blood vessel angles

Measurements of the major temporal retinal blood vessels angles were performed on the RNFL deviation maps. The intersections of the major superotemporal artery and inferotemporal artery with the 3.46 mm OCT measurement circle were manually determined by one investigator (KQ). Subsequently, we determined the retina artery angle, defined as the distance between the corresponding crossings in degrees along the circle (Figure 1B).

Definitions of disc ovality Index, disc torsion, horizontal and vertical disc tilt

The definitions of optic disc torsion and optic disc tilt have been described previously (Park et al., 2012; Takasaki et al., 2013). Briefly, Disc torsion degree was defined as the deviation of the long axis of the optic disc from the vertical reference (a vertical line 90° from a horizontal line connecting the disc center and the fovea). The angle between the longest axis of the optic disc and the vertical reference was determined as the torsion degree. An inferotemporal direction torsion (counterclockwise torsion in the right eye format) was presented as a positive value, while a superonasal direction torsion (clockwise torsion in the right eye format) was presented as a negative value. Optic disc tilt was determined as the tilt index (defined as the shortest diameter divided by the longest diameter).

The measurements of horizontal and vertical disc tilt were performed manually on HRT printouts with the ImageJ software (Takasaki et al., 2013). The horizontal disc tilt was defined as the angle subtended by a horizontal line and a line that was drawn to connect the two points where the height profile and the disc margin met (Fig. 2). The vertical disc tilt was defined as the angle subtended by the vertical line and the line joining the two points where the height profile and the disc margin met (Fig. 2). Horizontal disc tilt in temporal direction and downward vertical disc tilt in inferior direction were presented as positive angles. Nasal disc tilt and superior disc tilt were presented as negative angles.

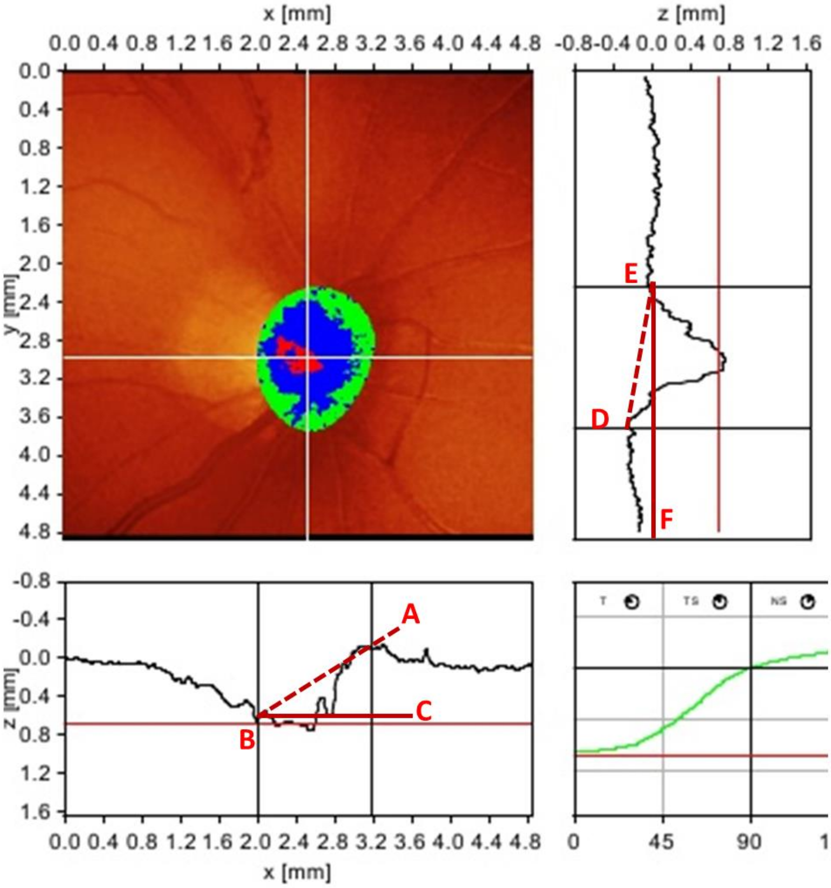

Figure 2. Measurements of horizontal and vertical disc tilt angles on HRT 2 printouts with the ImageJ software. Horizontal tilt angle (∠ABC=31.1°, temporal disc tilt) was defined as the angle between the horizontal line and a line (dashed) connecting the two points where the height profile and the disc margin met. Vertical tilt angle (∠DEF=-9.5°, upward disc tilt) was defined as the angle between the vertical line and a line (dashed) connecting the two points where the height profile and the disc margin met.

Statistical Analysis

The statistical analyses were performed with the SPSS software (ver. 23.0; SPSS Inc, Chicago, IL). Differences in RNFL thickness and the rim area among the 4 quadrants were analyzed using the 1-way analysis of variance with Tukey multiple comparison tests. The compliance of the ISNT rule and 2 variants (IS and IST rules) on RNFL thickness and rim area was determined and compared between two groups with a chi-square test. The effects of ocular factors (including axial length, disc area, disc tilt, disc torsion, DFA, and retina artery angle) on the performance of ISNT rules were evaluated with logistic regression analysis. A p value less than 0.05 was considered statistically significant.

Results

After excluding 9 subjects (6 subjects with unreliable visual field tests, and 3 subjects with poor OCT scan quality), one hundred and thirty eight eyes from 138 subjects (60 females and 89 right eyes) were finally included in the analysis. Table 1 presents the demographics of the study population. The mean age was 23.1±4.1 years (range, 18 to 40). The mean axial length and refractive error were 25.57±1.09 mm (range, 22.52 to 28.77 mm) and -5.12±2.30 D (range, -9.63 to -0.50 D), respectively. The mean average RNFL thickness and global rim area were 97.7±8.9 μm (range, 81 to 128μm) and 1.53±0.31mm^2 (range, 0.90 to 2.43 mm^2), respectively.

The rim area measured with HRT2 was greatest in the inferior quadrant, followed by the superior quadrant, the nasal quadrant, and the temporal quadrant (one way ANOVA, all with $p<0.001$). In 132 (95.7%) eyes, the temporal rim area was thinnest; in 4 (2.9%) eyes, the nasal rim area was thinnest; in 2 (1.4%) eyes, the superior rim area was thinnest. The IS (I > S), IST (I > S > T), and ISNT (I > S > N > T) rules were followed in 92 (66.7%) eyes, 90 (65.2%) eyes, and 87 (63.0%) eyes, respectively. A subgroup analysis revealed that no significant different compliance of ISNT rules was detected between high myopia and low to moderate myopia (Table 2A). Table 3 and Table 5 demonstrate the univariate logistic regression analysis and the corresponding multiple logistic regression results. After adjusting for the other covariates, disc area was found to be the only significant factor associated with the compliance of IS rule (odds ratio: 0.46, p=0.039), IST rule (odds ratio: 0.46, p=0.037), and ISNT rule (odds ratio: 0.44, p=0.030).

Table 1. Characteristics of the study population (n=138)

	Mean±SD	Range
Age, y	23.1±4.1	18 to 40
Spherical equivalent, D	-5.21±2.41	-15.75 to -0.50
Axial length, mm	25.60±1.12	22.52 to 28.77
Disc area (HRT2), mm^2	1.90±0.49	0.92 to 3.63
DFA, deg	5.5±3.1	-1.1 to +15.8
Artery angle, deg	65.4±10.5	38.3 to 88.5
Index of tilt	0.82±0.08	0.60 to 1.00
Disc torsion degree, deg	4.7±25.3	-77.4 to 87.1
Horizontal disc tilt angle, deg	14.9±7.6	-2.4 to 36.9
Vertical disc tilt angle, deg	2.1±6.3	-10.4 to 56.6
OCT RNFL measurements		
Average RNFL thickness, µm	97.7±8.9	81.0 to 128.0
Superior RNFL thickness, µm	118.6±17.4	79.0 to 191.0
Nasal RNFL thickness, µm	64.6±10.9	40.0 to 91.0
Inferior RNFL thickness, µm	123.3±17.6	81.0 to 175.0
Temporal RNFL thickness, µm	84.2±15.7	51.0 to 135.0
HRT2 rim area measurements		
Global rim area, mm^2	1.53±0.31	0.90 to 2.43
Superior rim area, mm^2	0.43±0.09	0.27 to 0.67
Nasal rim area, mm^2	0.39±0.10	0.19 to 0.73
Inferior rim area, mm^2	0.45±0.09	0.27 to 0.69
Temporal rim area, mm^2	0.26±0.08	0.12 to 0.61

Table 2. Percentage of eyes that comply with ISNT rules in high myopia and low to moderate myopia

	Mild to moderate myopia (n=91)	High myopia (n=47)	χ^2 test, p
A. HRT rim area			
IS rule	60 (65.9%)	32(68.1%)	0.85
IST rule	59 (64.8%)	31(66.0%)	0.99
ISNT rule	58 (63.7%)	29(61.7%)	0.85
B. OCT RNFL thickness			
IS rule	63 (69.2%)	28(59.6%)	0.26
IST rule	59 (64.8%)	21(44.7%)	0.03
ISNT rule	12 (13.2%)	4(8.5%)	0.58

Table 3. Factors associated with performance of IS, IST, and ISNT rules on rim area obtained with HRT2 (n=138; univariate logistic regression analysis)

	IS rule		IST rule		ISNT rule	
	Odds ratios (95%CI)	p	Odds ratios (95%CI)	p	Odds ratios (95%CI)	p
Gender	1.00(0.49-2.04)	1.000	1.16(0.57-2.34)	0.684	1.26(0.63-2.53)	0.516
Age	0.99(0.91-1.08)	0.857	1.00(0.92-1.10)	0.928	0.99(0.92-1.08)	0.935
Axial length	0.91(0.66-1.25)	0.550	0.89(0.65-1.22)	0.470	0.88(0.65-1.21)	0.431
Artery angle	1.01(0.99-1.03)	0.395	1.01(0.99-1.03)	0.406	1.01(0.99-1.03)	0.338
DFA	1.03(0.92-1.15)	0.624	1.03(0.92-1.16)	0.558	1.04(0.93-1.16)	0.204
Disc area	0.55(0.27-1.12)	0.098	0.46(0.23-0.96)	0.037	0.53(0.26-1.07)	0.076
Index of tilt	0.07(0.01-6.86)	0.259	0.04(0.01-3.45)	0.155	0.18(0.01-14.65)	0.446
Disc torsion degree	0.99(0.98-1.01)	0.644	0.99(0.97-1.01)	0.128	0.99(0.97-1.01)	0.214
Horizontal tilt angle	1.01(0.97-1.06)	0.596	1.02(0.97-1.06)	0.524	0.99(0.95-1.05)	0.941
Vertical tilt angle	0.95(0.89-1.02)	0.139	0.96(0.90-1.02)	0.213	0.95(0.89-1.02)	0.150

Table 4. Factors associated with performance of IS and IST rules on RNFL thickness obtained with SD-OCT (n=138; univariate logistic regression analysis)

	IS rule		IST rule	
	Odds ratios (95%CI)	p	Odds ratios (95%CI)	p
Gender	0.94(0.46-1.92)	0.875	1.10(0.56-2.17)	0.785
Age	1.07(0.96-1.18)	0.212	1.09(0.98-1.20)	0.093
Axial length	0.98(0.72-1.35)	0.909	0.72(0.52-0.98)	0.040
Artery angle	0.99(0.97-1.02)	0.618	1.02(0.99-1.04)	0.058
DFA	1.30(1.13-1.50)	<0.001	1.19(1.05-1.34)	0.006
Disc area	0.77(0.38-1.56)	0.461	1.64(0.81-3.34)	0.171
Index of tilt	0.22(0.01-19.00)	0.503	13.61(0.18-102.08)	0.236
Disc torsion degree	1.00(0.98-1.02)	0.884	1.00(0.98-1.03)	0.498
Horizontal tilt angle	1.03(0.98-1.08)	0.257	0.98(0.93-1.02)	0.317
Vertical tilt angle	1.00(0.95-1.07)	0.806	0.97(0.91-1.03)	0.344

Table 5. Factors associated with performance of IS, IST and ISNT rules on RNFL thickness and rim area obtained with SD-OCT and HRT2 (n=138; multiple logistic regression analysis) (backward method, variable enter if p <0.20, variable remove if p>0.1)

	Odds ratios (95%CI)	p
IS rule (OCT)		
DFA	1.30(1.13-1.50)	<0.001
IST rule (OCT)		
DFA	1.20(1.06-1.35)	0.005
Disc area	1.91(0.91-4.04)	0.089
Axial length	0.75(0.54-1.03)	0.078
IS rule (HRT2)		
Disc area	0.46(0.22-0.96)	0.039
Vertical tilt angle	0.93(0.86-1.01)	0.080
IST rule (HRT2)		
Disc area	0.46(0.23-0.96)	0.037
ISNT rule (HRT2)		
Disc area	0.44(0.21-0.92)	0.030
Vertical tilt angle	0.94(0.86-1.01)	0.080

On average, the RNFL thickness measurement obtained with SD-OCT was thickest in the inferior quadrant, followed by the superior quadrant, temporal quadrant, and the nasal quadrant (one way ANOVA, all with $p<0.001$). In 119 (85.6%) eyes, the nasal RNFLwas thinnest; in 19 (14.4%) eyes, the temporal RNFL was thinnest. Regarding the ISNT rule and the two variants, 91(65.9%) eyes complied with the IS rule, while 80 (58.0%) eyes complied with the IST rule. However, the ISNT rule was followed in only 16 (11.6 %) eyes. In the subgroup analysis, lower percentage of eyes in high myopia group were found to comply with the IST rule than that of low to moderate myopia (44.7% vs 64.8%, $p=0.03$). No significant different compliance of IS rule and ISNT rule was found between the two groups (Table 2B). Table 4 demonstrates the potential factors associated with the performance of the IS and IST rules by using univariate logistic regression analysis. As most of the eyes (88.4%) violated the ISNT rule, the ISNT rule was not included in this analysis. DFA was significantly associated with the performance of IS and IST rules (odds ratio: 1.30, $p<0.001$; odds ratio: 1.19, $p=0.006$, respectively). Axial length (odds ratio: 0.72, $p=0.040$) and retina artery angle (odds ratio: 1.02, $p=0.058$) were found to correlate with the compliance of IST rule. In the multiple analysis, DFA was the only significant factor associated with the compliance of IS rule and IST rule, after adjusting for other covariates (Table 5).

Discussion

In the present study, we evaluated the application of the ISNT rules on retina nerve fiber layer thickness and neuroretinal rim area in healthy myopic eyes by using SD-OCT and HRT2. Although the performance of ISNT rule on rim area was better than on RNFL thickness, 88.4% and 37% of eyes did not comply with the ISNT rule on RNFL thickness and rim area, respectively. For rim area, smaller disc area was significantly associated with increased compliance of the IS, IST and ISNT rules. For RNFL thickness, greater DFA was significantly associated with increased compliance of the IS and IST rules.

Previous studies have evaluated the performance of ISNT rule on rim area (Sihota et al., 2008; Morgan et al., 2012; Chan et al., 2013; Dave & Shah 2015; Pradhan et al., 2016). By using optic disc photographs, 46% to 79% of the eyes were reported to follow the ISNT rule (Harizman et al., 2006; Wang et al., 2007; Law et al., 2016). By using CSLO, the ISNT rule was applicable in 71% of 136 normal eyes (Sihota et al., 2008). However, significant low compliance of ISNT rule was also reported in several studies (Iester et al., 2011; Chan et al., 2013; Nayak et al., 2015). In a population based study, Chan et al. (2013) reported that only 15.7% of nonglaucomatous eyes obeyed the ISNT rule on rim area obtained with HRT3. In another study, Natasha et al. (2015) evaluated the ISNT rule fulfillment in a Caucasian normative database consisting of 280 subjects by using HRT3. They found that 18% of normal eyes had rim areas that complied with the ISNT rule. In the present study, however, we found that ISNT rule was intact in a majority of myopic eyes (63%). Several differences in study design could have contributed to these conflicting results, such as different study population and different measurement methods of rim area. For example, only myopic eyes were included in the present study while normal eyes were analyzed in previous studies. The mean disc area in our study was 1.90 mm^2, which was smaller than that of Natasha's study (2.40mm^2) (Nayak et al., 2015). Disc size has been reported to have influence on rim area measurement (Oddone et al., 2009). Moreover, disc area was reported to be associated with the performance of ISNT rule (Chan et al., 2013; Nayak et al., 2015). Consistent with previous studies (Chan et al., 2013; Nayak et al., 2015), we found that smaller disc area was significantly associated with increased compliance of IS, IST, and ISNT rules. Although axial length has been reported to correlate with rim area in previous studies (Cheung et al., 2011; Savini et al., 2012), no significant difference in compliance of ISNT rules between high myopia and low to moderate myopia groups was detected in current study. Optic disc torsion and disc tilt have been reported to correlate with rim area measurement (Tong et al., 2007; Arvind et al., 2008). In the present study, however, optic disc torsion, disc tilt and retinal artery angle were not associated with the performance of ISNT rules.

Although the ISNT rule was generally used to characterize the normal neuroretinal rim (Jonas et al., 1988; Jonas et al., 1998), we also evaluated the compliance of the ISNT rule on RNFL thickness in myopic eyes. Previous studies have already reported the variability of ISNT rule fulfilment on RNFL thickness in normal eyes (Alasil et al., 2013; Dave & Shah 2015; Pradhan et al., 2016). By using the time-domain OCT, Pradhan et al. (2016) reported that 47.1% and 58.7% of normal eyes obeyed the ISNT rule and IST rule, respectively. In another study, Dave et al. found that 55% and 58.7% of normal eyes obeyed the ISNT rule and IST rule on RNFL thickness, respectively (Dave & Shah 2015). Compared with previous studies (Dave & Shah 2015; Pradhan et al., 2016), we found significant low compliance of ISNT rule in myopic eyes. Only 11.6% of eyes obeyed the ISNT rule on RNFL thickness in the present study. One possible explanation is that myopic eyes have different RNFL distribution compared with normal eyes. Increased temporal RNFL thickness in myopic eyes has been reported previously (Wang et al., 2011; Leung et al., 2012). In line with previous studies (Wang et al., 2011; Leung et al., 2012), we found that temporal RNFL thickness was significantly thicker than nasal RNFL thickness in the current study population. Moreover, we found nasal RNFL thickness but not temporal thickness was thinnest in most of the myopic eyes (85.6%). Thus, one would not feel surprise to find the low compliance of ISNT rule in the current myopic population. For the two variants of ISNT rule on RNFL thickness, we found that 65.9% and 58.0% of healthy myopic eyes were compliant with the IS and IST rules, respectively. This is similar to previous reported results (Dave & Shah 2015; Pradhan et al., 2016).

Previously, myopia status has been reported to be associated with RNFL distribution (Leung et al., 2012; Pereira et al., 2015). In the current study, we found that lower percentage of eyes in high myopia group was compliant with the IST rule than that of low to moderate myopia group (44.7% vs 64.8%, p=0.03). Correspondingly, shorter axial length was associated with increased compliance of IST rule in the univariate logistic regression analysis (Table 4). After adjusting other covariates, however, DFA but not axial length was significantly associated with the performance of IS and IST rules. The result of the current study fits well with previous studies regarding the association between DFA and RNFL distribution (Amini et al., 2014; Choi et al., 2014). Choi et al. (2014) reported that greater DFA was significantly associated with increased inferior RNFL thickness and decreased superior RNFL thickness in healthy myopic eyes. Although retinal vascular pattern and optic disc anatomy (disc tilt, disc torsion, etc) have been reported to correlate with RNFL distribution in previous studies (Pereira et al., 2015; Shin et al., 2015), we did not detect any significant association between retina artery angle, disc tilt, disc torsion degree and the compliance of IS and IST rules.

In the present study, the application of the ISNT rule was only evaluated in healthy subjects as we did not include glaucoma subjects. For good glaucoma diagnostic performance in clinical practice, however, the ISNT rule should be not only obeyed in the majority of healthy eyes but also violated in the majority of eyes with glaucoma. Thus, it is important to evaluate the performance of ISNT rule in myopic eyes with glaucoma. By using optic disc photographs, Kim et al. (2014) reported that the sensitivity and specificity of the ISNT rule in diagnosing glaucomatous eyes with myopic titled discs were 73.3% to 75.7% and 68.3% to 71.4%, respectively. Future studies are needed to evaluate the diagnostic performance of ISNT rule on rim area and RNFL thickness obtained with HRT and OCT in myopic population.

One of the limitations of the current study is that only young myopic subjects were included. Age related decrease in global rim area and average RNFL thickness has been reported in previous studies (Cheung et al., 2011; Alasil et al., 2013). However, previous studies have found no significant effect of age on compliance of ISNT rules (Harizman et al., 2006; Wang et al., 2007; Nayak et al., 2015). Another limitation is that ocular magnification for OCT measurement was not adjusted in the present study. However, ocular magnification is likely to have similar effect on RNFL measurement of the 4 quadrants because of the extending nature of peripapillary retinal nerve fibers. Thus, ocular magnification may not have great effect on the distribution of peripapillary RNFL thickness. Other limitations are that this was not a population-based study and that it involved only Chinese subjects. Thus, the current findings may not apply to other populations.

In conclusion, 88.4% and 37% of the healthy myopic eyes did not comply with the ISNT rule on RNFL thickness and rim area, respectively. For rim area measurement, smaller disc area was significantly associated with increased compliance of the ISNT, IST and IS rules. For RNFL thickness, greater DFA was significantly associated with increased compliance of the IS and IST rules. Due to significant low compliance in healthy eyes, the ISNT rule and its variants have limited potential utility in diagnosing glaucoma in myopic subjects.

Reference

Alasil T, Wang K, Keane PA, Lee H, Baniasadi N, de Boer JF & Chen TC (2013): Analysis of normal retinal nerve fiber layer thickness by age, sex, and race using spectral domain optical coherence tomography. J Glaucoma. 22: 532-541.

Amini N, Nowroozizadeh S, Cirineo N, et al (2014): Influence of the disc-fovea angle on limits of RNFL variability and glaucoma discrimination. Invest Ophthalmol Vis Sci. 55: 7332-7342.

Arvind H, George R, Raju P, Ve RS, Mani B, Kannan P& Vijaya L (2008): Neural rim characteristics of healthy South Indians: the Chennai Glaucoma Study. Invest Ophthalmol Vis Sci. 49: 3457-3464.

Chan EW, Liao J, Wong R, Loon SC, Aung T, Wong TY & Cheng CY (2013): Diagnostic Performance of the ISNT Rule for Glaucoma Based on the Heidelberg Retinal Tomograph. Transl Vis Sci Technol. 2: 2.

Cheung CY, Chen D, Wong TY, et al (2011): Determinants of quantitative optic nerve measurements using spectral domain optical coherence tomography in a population-based sample of non-glaucomatous subjects. Invest Ophthalmol Vis Sci. 52:9629-9635.

Choi JA, Kim JS, Park HY, Park H & Park CK (2014): The foveal position relative to the optic disc and the retinal nerve fiber layer thickness profile in myopia. Invest Ophthalmol Vis Sci. 55: 1419-1426.

Dave P & Shah J (2015): Applicability of ISNT and IST rules to the retinal nerve fibre layer using spectral domain optical coherence tomography in early glaucoma. Br J Ophthalmol. 99: 1713-1717.

Fallon M, Valero O, Pazos M & Antón A (2017): Diagnostic Accuracy of Imaging Devices in Glaucoma: A Meta-Analysis. Surv Ophthalmol. 62: 446-461.

Harizman N, Oliveira C, Chiang A, Tello C, Marmor M, Ritch R & Liebmann JM (2006): The ISNT rule and differentiation of normal from glaucomatous eyes. Arch Ophthalmol 124: 1579-1583.

Hwang YH & Kim YY (2015): Application of the ISNT Rule to Neuroretinal Rim Thickness Determined Using Cirrus HD Optical Coherence Tomography. J Glaucoma. 24: 503-507.

Iester M, Bertolotto M, Recupero SM & Perdicchi A (2011): The "ISN'T rule" in healthy participant optic nerve head by confocal scanning laser ophthalmoscopy. J Glaucoma. 20: 350-354.

Jonas JB, Budde WM & Lang P (1998): Neuroretinal rim width ratios in morphological glaucoma diagnosis. Br J Ophthalmol. 82:1366-1371.

Jonas JB, Gusek GC & Naumann GO (1988): Optic disc, cup and neuroretinal rim size, configuration and correlations in normal eyes. Invest Ophthalmol Vis Sci. 29:1151-1158.

Kim MJ, Kim SH, Hwang YH, Park KH, Kim TW & Kim DM (2014): Novel screening method for glaucomatous eyes with myopic tilted discs: the crescent moon sign. JAMA Ophthalmol. 132: 1407-1413.

Law SK, Kornmann HL, Nilforushan N, Moghimi S & Caprioli J (2016): Evaluation of the "IS" Rule to Differentiate Glaucomatous Eyes From Normal. J Glaucoma. 25: 27-32.

Leung CK, Yu M, Weinreb RN, Mak HK, Lai G, Ye C & Lam DS (2012). Retinal nerve fiber layer imaging with spectral-domain optical coherence tomography: interpreting the RNFL maps in healthy myopic eyes. Invest Ophthalmol Vis Sci. 53: 7194-7200.

Marcus MW, de Vries MM, Junoy Montolio FG & Jansonius NM (2011): Myopia as a risk factor for open-angle glaucoma: a systematic review and meta-analysis. Ophthalmology. 118: 1989-1994.e2.

Morgan IG, Ohno-Matsui K & Saw SM (2012). Myopia. Lancet . 379: 1739-1748.

Morgan JE, Bourtsoukli I, Rajkumar KN, Ansari E, Cunliffe IA, North RV & Wild JM (2012): The accuracy of the inferior>superior> nasal>temporal neuroretinal rim area rule for diagnosing glaucomatous optic disc damage. Ophthalmology 119: 723-730.

Nayak NV, Berezina TL, Fechtner RD, Sinai MJ & Khouri AS (2015): Effect of age and disc size on rim order rules by Heidelberg Retina Tomograph. J Glaucoma. 24: 377-382.

Oddone F, Centofanti M, Iester M, Rossetti L, Fogagnolo P, Michelessi M, Capris E & Manni G (2009): Sector-based analysis with the Heidelberg Retinal Tomograph 3 across disc sizes and glaucoma stages: a multicenter study. Ophthalmology. 116:1106-1111.e1-3.

Park HY, Lee K & Park CK (2012): Optic disc torsion direction predicts the location of glaucomatous damage in normal-tension glaucoma patients with myopia. Ophthalmology. 119:1844-1851.

Pereira I, Resch H, Schwarzhans F, et al (2015): Multivariate Model of the Intersubject Variability of the Retinal Nerve Fiber Layer Thickness in Healthy Subjects. Invest Ophthalmol Vis Sci. 56:5290-5298.

Pradhan ZS, Braganza A & Abraham LM (2016): Does the ISNT Rule Apply to the Retinal Nerve Fiber Layer? J Glaucoma. 25:e1-4.

Savini G, Barboni P, Parisi V & Carbonelli M (2012): The influence of axial length on retinal nerve fibre layer thickness and optic-disc size measurements by spectral-domain OCT. Br J Ophthalmol. 96: 57-61.

Shin HY, Park HY & Park CK. The effect of myopic optic disc tilt on measurement of spectral-domain optical coherence tomography parameters. Br J Ophthalmol. 2015 Jan;99(1):69-74.

Sihota R, Srinivasan G, Dada T, Gupta V, Ghate D & Sharma A (2008): Is the ISNT rule violated in early primary open-angle glaucoma – a scanning laser tomography study. Eye (Lond) 22: 819-824.

Takasaki H, Higashide T, Takeda H, Ohkubo S & Sugiyama K (2013): Relationship between optic disc ovality and horizontal disc tilt in normal young subjects. Jpn J Ophthalmol. 57: 34-40.

Tong L, Chan YH, Gazzard G, et al (2007): Heidelberg retinal tomography of optic disc and nerve fiber layer in singapore children: variations with disc tilt and refractive error. Invest Ophthalmol Vis Sci. 48:4939-4944.

Wang G, Qiu KL, Lu XH, Sun LX, Liao XJ, Chen HL & Zhang MZ (2011): The effect of myopia on retinal nerve fibre layer measurement: a comparative study of spectral-domain optical coherence tomography and scanning laser polarimetry. Br J Ophthalmol. 95:255-260.

Wang Y, Xu L & Jonas JB (2007): Shape of the neuroretinal rim and its correlations with ocular and general parameters in adult Chinese: the Beijing eye study. Am J Ophthalmol 144: 462-464.